

Insoluble anode of porous lead dioxide for electrosynthesis: preparation and characterization

N. MUNICHANDRAIAH, S. SATHYANARAYANA

Department of Inorganic and Physical Chemistry, Indian Institute of Science, Bangalore 560 012, India

Received 26 July 1985; revised 1 October 1985

Preparation of a novel type of titanium-substrate lead dioxide anode with enhanced electrocatalytic activity for electrosynthesis is described. It has been demonstrated that in the presence of a suitable surfactant in the coating solution, an adherent and mainly tetragonal form of lead dioxide is deposited on a platinized titanium surface such that the solution side of the coating is porous while the substrate side is compact. By an analysis of anodic charging curves and steady-state Tafel plots with such porous electrodes in contact with sodium sulphate solution, it has been proved that the electrochemically active area of these anodes is higher by more than an order of magnitude when compared to the area of conventional titanium-substrate lead dioxide anodes. The electrocatalytic activity is also thereby enhanced to a significant degree.

1. Introduction

One of the important components for electro-synthetic applications is the anode material which should, firstly, be stable under conditions of anodic polarization, i.e. should function as an insoluble anode. Secondly, it should be a sufficiently good electrocatalyst for the desired reaction. Finally, it should be economical for production and use.

The choice of insoluble anodes is limited to (a) graphite which, however, is subjected to fairly strong erosion under anodic conditions; (b) noble metals (e.g. platinum, palladium, ruthenium, iridium) or their oxides; and (c) oxides of certain non-noble metals which are partially or fully conducting (e.g. Co_3O_4 , MnO_2 , PbO_2).

The base metal oxides mentioned above in (c) are of particularly technological importance as insoluble anodes due to their inherently low cost. Their relatively weak mechanical strength, however, necessitates the use of a conducting support such as titanium, which should have sufficient corrosion resistance under open circuit and a passivation tendency under anodic conditions.

The use of a conducting support leads, primarily, to a new problem, namely that of

adhesion between the support and the coating, without causing any significant ohmic drop. Inadequate adhesion leads to a flake-off of the coating and a build-up of a barrier layer of the valve metal oxide between the support and the electrocatalytic coating, rendering the anode eventually useless.

The second problem which arises with the use of the base metal oxide anodes is that of enhancing the surface area of the oxide without making it powdery, because a powdery structure is liable to intense shedding under conditions of anodic gas evolution. If fine particles of the oxide are rigidized with a binder, there is little chance of success since inorganic binders will usually be non-conducting and cause an ohmic drop in the electrode (with attendant problems), while organic binders will be oxidized to carbon dioxide etc.

In the present work a new process has been developed to overcome the above problems, and has been applied to the preparation of insoluble anodes of β -lead dioxide with a fine pore structure on the outer surface (i.e. solution side), low porosity on the inner surface (i.e. substrate side), strong adhesion to titanium substrate and good cohesion within the coating. The process used to prepare these electrodes and methods employed

to characterize them by anodic charging curves and Tafel plot analysis are described.

2. Previous work on lead dioxide electrodes

Lead dioxide has found extensive applications as a reducible cathode in the conventional lead–acid storage battery. It is useful to separate the preparation and properties of lead dioxide as a reducible cathode [1–4] from the characteristics of lead dioxide as a non-oxidizable anode considered here.

Composite electrodes of lead dioxide deposited on titanium for use as insoluble anodes have been described and reviewed in the literature [5–14]. Usually, the process involves the anodic deposition of lead dioxide on a pre-conditioned and, sometimes, noble metal-plated surface of titanium from an aqueous acidic solution of a lead(II) salt. The product thus obtained may generally be described as a coating of the relatively non-adherent and non-porous β -form of lead dioxide with considerable internal stress on a titanium surface.

The β -form of lead dioxide has a tetragonal, rutile-like structure and may be expected to form a solid solution with the TiO_2 (rutile) film on titanium. This should obviate the need for any other conductive undercoat to the PbO_2 coating and also provide a good bonding with the titanium substrate.

Earlier literature, however, indicates that a suitable undercoat to the PbO_2 layer on titanium is necessary [11, 15] to overcome premature failure caused, perhaps, by the presence of some orthorhombic (α -form) PbO_2 (which seems unavoidable [16]), and which thereby permits an interstitial diffusion of oxygen through the PbO_2 layer [17] up to the bare titanium surface, thus oxidizing the latter [15]. Another failure mechanism identified involves dissolution of PbO_2 as Pb^{4+} under anodic polarization in strong acid solutions [18].

It is common practice in the literature on PbO_2 anode preparation to aim at conditions which produce a compact or 'pin-hole free' deposit. The implications are that the use of a non-compact PbO_2 coating may lead to an oxidative degradation of the PbO_2 walls inside the pores (in analogy with the failure mode of

porous graphite anodes in chloralkali cells) and an oxidative degradation of the titanium surface through anodic reaction with the solution in the pores (in analogy with the failure mode of PbO_2 -coated titanium anodes without any conducting intermediate layer).

These anticipated problems are either non-existent or avoidable, firstly because there is no higher oxidation state for PbO_2 (unlike CO_2 for carbon-based anodes) which could sustain an oxidative degradation of the coating, and secondly because the incorporation of an intermediate layer (platinum in the present work) between the titanium and the lead dioxide serves as a barrier to the diffusion of oxygen, thus eliminating any significant oxidation of the titanium surface.

In the case of ruthenium oxide-coated titanium substrate anodes it is known, for example, that a microcracked surface is highly desirable both with regard to low effective current density and long operational life [19].

3. Present work

It is reasonable to expect that a PbO_2 coating with proper porosity and a non-porous, conducting undercoat will be not only devoid of any serious life-limiting problem but also provide an enhanced area for anodic reactions. The increase in area will have several advantages: lower effective current density and hence lower anode potential and wear rate, as well as a lower possibility of side reactions.

The required porosity is best obtained by controlling the crystal growth of β -lead dioxide during its anodic deposition, which then provides a high degree of cohesion to the deposit without any binder material. These results have been achieved in the present work by addition to the PbO_2 coating solution of a foaming agent, Teepol (a mixture of sodium sec.-alkyl sulphates, $\text{C}_n\text{H}_{2n+1}\text{CH}(\text{CH}_3)\text{OSO}_3\text{Na}$, where $n = 6$ to 16).

4. Experimental details

4.1. Chemicals

Reagent grade chemicals were used throughout.

Solutions were prepared with twice-distilled water. Presaturation of test solutions with hydrogen or oxygen was carried out by passing the corresponding gas obtained from an all-glass electrolyser through suitable purifying columns and then through the test solution.

4.2. Preparation of anodes

Strips (12×20 mm with stem length 100 mm) were cut from titanium sheet (2.5 mm thick) of commercial purity (ASTM grade B-265). The strips were abraded with emery, degreased in alkali, etched in hot sulphuric acid, electroplated with platinum ($\sim 5 \mu\text{m}$) and anodically polarized in a solution containing $250 \text{ g l}^{-1} \text{ Pb}(\text{NO}_3)_2$, $50 \text{ g l}^{-1} \text{ Cu}(\text{NO}_3)_2 \cdot 3\text{H}_2\text{O}$ and $0.5 \pm 0.1 \text{ g l}^{-1}$ Teepol, at $60 \pm 2^\circ \text{C}$. The initial current density of 50 mA cm^{-2} was applied for 1 min, followed by a current density of 20 mA cm^{-2} for such a time as to obtain a coating of PbO_2 , 0.5 mm or 1.0 mm thick, using a copper cathode and keeping the pH of the solution constant by periodical addition of $\text{PbCO}_3 + \text{CuCO}_3$ (1:1). The coated anodes were thoroughly washed and dried at 60°C .

For comparison, PbO_2 coating on a platinum-plated titanium substrate was also made by electrodepositing from a solution of the composition stated above but not containing any surfactant additive. The product in this case was a compact or non-porous coating of PbO_2 .

For clarity, the two types of electrodes obtained above are designated as 'porous $\beta\text{-PbO}_2(\text{Ti})$ electrode' and 'compact $\beta\text{-PbO}_2(\text{Ti})$ electrode' for the PbO_2 coating from solution with and without Teepol, respectively.

4.3. Physical studies on the oxide anodes

X-ray studies and SEM examinations were carried out with standard commercial units. BET surface area measurements were also attempted, but these were unsuccessful with the as-prepared electrodes due to their relatively low specific surface. On the other hand, powdered samples with their high specific surface were not considered relevant as they do not correspond to the actual situation involved in the use of oxide anodes.

4.4. Electrochemical studies on the oxide anodes

Open-circuit potentials, galvanostatic charging curves and steady-state anodic Tafel plot measurements were made with several samples of porous $\beta\text{-PbO}_2(\text{Ti})$ and compact $\beta\text{-PbO}_2(\text{Ti})$ anodes of thickness 0.5 and 1.0 mm.

The cell used for the electrochemical characterization of the oxide anodes was of all-glass construction, as shown in Fig. 1. The temperature of the cell was maintained at $40 \pm 1^\circ \text{C}$ by immersing the cell in a water thermostat. A regulated power supply with adjustable high resistance elements in series with the cell was used to obtain galvanostatic charging curves, as well as steady-state polarization curves. In the latter studies the working electrode was assumed to have attained a steady state when any drift of its electrode potential was 0.05 mV min^{-1} or less. A silicon diode with low reverse current characteristic was inserted in series with the cell in order to prevent any inadvertent cathodic polarization of the PbO_2 electrode.

Anodic galvanostatic charging curves were always taken after presaturating the solution with oxygen and attaining a steady state under open-circuit condition. Tafel polarization curves were also recorded point by point after presaturating the solution with oxygen and ensuring, in addition, that a steady state was reached for each current. Open-circuit potentials were measured in the steady state as a function of pH of the solution in both oxygen-saturated and hydrogen-saturated solutions. The pH of the solution was adjusted in each case by adding dilute H_2SO_4 or dilute NaOH as required.

The derivatives of the charging curves, which are required for the determination of the differential capacity of the double layer at the working electrode-solution interface, were obtained by graphical differentiation of the charging curves. Thus, the experimental charging curves were first plotted on a large-scale graph and a smooth best-fit curve was obtained. A plane metal mirror was aligned at the chosen point on the curve to locate the normal to the tangent at that point. By reading off the coordinates at the intersection of the axes by the edges of the mirror, the derivatives were calculated with an accuracy of about 1%.

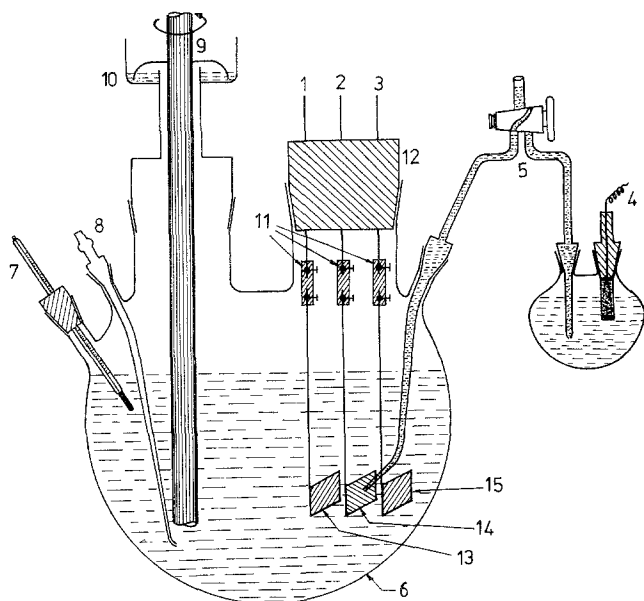


Fig. 1. Schematic view of the cell used for electrochemical studies with β - $\text{PbO}_2(\text{Ti})$ anodes. 1, 2, 3, 11, electrode leads and screw connectors of titanium; 4, reference electrode; 5, salt bridge; 6, cell; 7, thermometer; 8, gas (H_2 or O_2) inlet; 9, stirrer; 10, water seal; 12, Teflon joint; 14, working electrode (PbO_2); 13, 15, counter electrodes (titanium).

5. Results and discussion

5.1. Action of Teepol

The primary mode of action of the Teepol additive is to partially stabilize the oxygen bubbles as they are formed on the growing surface of the PbO_2 until the bubbles grow large enough to escape. (The current efficiency for PbO_2 deposition is 65–95% depending on the concentration of the additive, the higher value applying when there is no additive in the solution.) As a result the external surface develops a large number of pores, approximately 100–500 μm in range. As will be proved below, this results in a 15 to 40-fold increase in the true area available for anodic reactions on the electrode. If the thickness of the PbO_2 coating is about 1 mm (or more), it is found that the porosity of the coating is nearly absent at the interior edge of the coating, which is also a desirable result. This takes place, apparently, because the growth of the deposit by overlap progressively reduces the porosity. The second important mode of action of the additive is to cause good wetting of the substrate by the solution so that the adhesion of the PbO_2 coating to the substrate is improved to a remarkable degree. Lastly, the mean size of PbO_2 crystallites is reduced in the presence of the surfactant due to adsorption of the latter on the

crystal nuclei. The smaller mean particle size enhances the true surface area available for electrochemical reaction and thereby decreases the overpotential at a given apparent current density.

5.2. Phase composition of the anode coating

The X-ray diagrams of the coating samples removed from unused anodes showed that the β -form of PbO_2 was the major component, with the α -form as a minor component. This agrees with the earlier findings of Mindt [16]. No attempt was made to eliminate the α -form completely by electrodepositing PbO_2 at lower pH values of the coating solution since this is unlikely to be successful [16] even from solutions at zero pH.

5.3. Porosity of the anode

The pore volume of the anode coating was determined by weighing the amount of water imbibed in the pores under controlled conditions and relating it to the gross volume of PbO_2 alone. The void volume in the anodes was thus found to be $12 \pm 2\%$ (different samples) for the porous β - $\text{PbO}_2(\text{Ti})$ anodes, and $1.5 \pm 0.5\%$ (different samples) for the compact β - $\text{PbO}_2(\text{Ti})$ anodes.

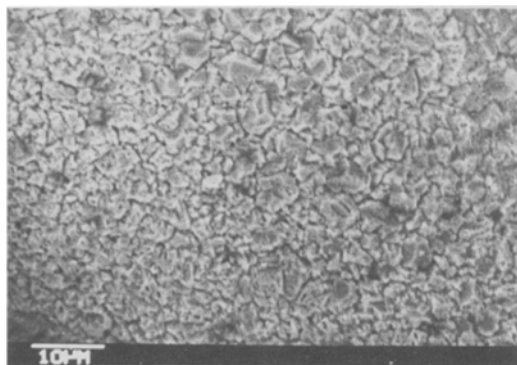


Fig. 2. SEM photograph showing grain structure of a porous β - $\text{PbO}_2(\text{Ti})$ electrode (with coating 1 mm thick).

5.4. SEM studies

These revealed that the grain structure was significantly finer in the case of porous β - $\text{PbO}_2(\text{Ti})$ coatings than in the case of compact β - $\text{PbO}_2(\text{Ti})$ coatings (Figs 2, 3). Further, the pores in the porous β - $\text{PbO}_2(\text{Ti})$ anode coatings were more like hemispherical cavities with a shallow depth than through-pores extending across the whole thickness of the coating. The larger cavities usually terminated in smaller cavities located at the bottom or sides of the cavity. Presumably, the small cavities terminate in similar, even smaller, cavities or closed ends (Figs 4–6).

5.5. Adhesion, hardness and internal stress

These were evaluated only qualitatively. The adhesion of the coating in the case of porous β - $\text{PbO}_2(\text{Ti})$ anodes was such that it was virtually

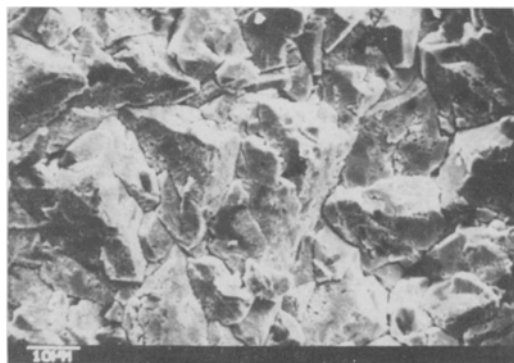


Fig. 3. SEM photograph showing grain structure of a compact β - $\text{PbO}_2(\text{Ti})$ electrode (with coating 1 mm thick).

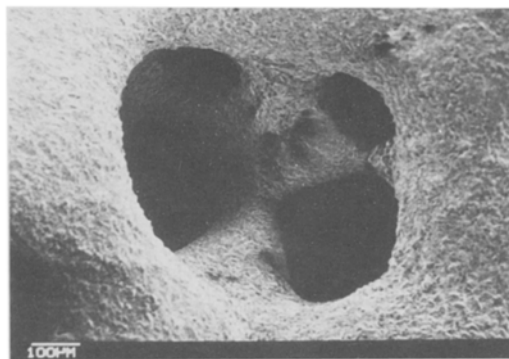


Fig. 4. SEM photograph showing wide but shallow pores on the exterior surface (i.e. solution side) of a porous β - $\text{PbO}_2(\text{Ti})$ electrode (with coating 1 mm thick).

impossible to separate it from the substrate without detaching the intermediate platinum layer, at least partially, unlike the case of compact β - $\text{PbO}_2(\text{Ti})$ anodes where the detachment was relatively easy. Scratch tests showed that the porous β - $\text{PbO}_2(\text{Ti})$ anodes were as hard or harder than compact β - $\text{PbO}_2(\text{Ti})$ anodes. The absence of longitudinal cracks in the coating or an absence of a tendency of the coating to flake-off in fairly long-term electrosynthesis studies (perchlorate from chlorate) indicated the absence of internal stress in the case of porous β - $\text{PbO}_2(\text{Ti})$ anodes. (The anode coatings were damaged when subjected to strong mechanical or thermal shock. This failure-mode is not, however, related to internal stress only.) This is to be expected since the presence of numerous minute cavities

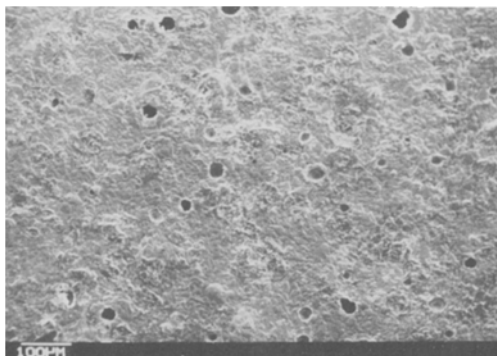


Fig. 5. SEM photograph showing minute pores on the interior surface (i.e. substrate side) of a porous β - $\text{PbO}_2(\text{Ti})$ electrode (with coating 1 mm thick). For this test the porous β - PbO_2 coating was detached from the substrate by tamping and wedging out with a knife edge, exposing the reverse side.



Fig. 6. SEM photograph of a β -PbO₂ layer (removed from a β -PbO₂(Ti) electrode) parallel to the growth direction. The substrate (titanium) is towards the right side of the figure.

facilitates the spontaneous relief of any internal stress to a large extent.

5.6. Electrochemical studies on the anodes

In order to characterize interfacial properties such as double-layer capacitance and electrochemically active area, it is necessary to minimize the flow of any faradaic current over as wide a range of polarization as possible (only anodic polarization is permissible in the present case) by a proper choice of the electrolyte solution. Preliminary studies with several solutions showed that, depending on the solution, the anode coating may be attacked (chloride solutions, alkaline solutions), or the solution may be contaminated with undesirable cathodic reduction products (chlorate solutions) etc., in many cases.

It was thus found that a solution of sodium sulphate permitted a wide range of anodic polarization with a high polarizability (i.e. low faradaic current densities) and permitting reproducible measurements with a given sample.

The electrochemical characterization of porous β -PbO₂(Ti) as well as compact β -PbO₂(Ti) electrodes was therefore carried out in a Na₂SO₄ (0.2 M) solution with regard to open-circuit behaviour, anodic charging transients and steady-state anodic polarization in the Tafel region.

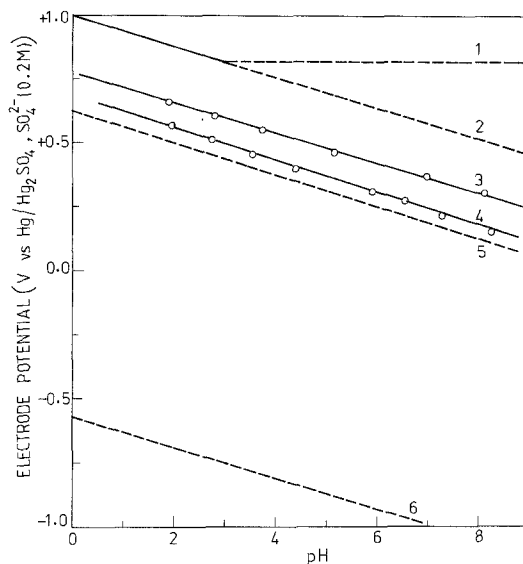
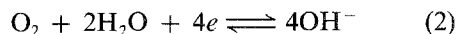
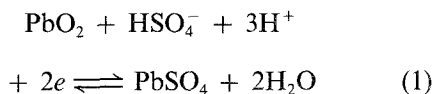


Fig. 7. The dependence of open-circuit potential of porous β -PbO₂(Ti) electrode on the pH of Na₂SO₄ solution. 1: β -PbO₂/PbSO₄, SO₄²⁻ (1.0 M), 25° C (experimental) [20]. 2: β -PbO₂/PbSO₄, SO₄²⁻ (1.0 M), 25° C (theory). 3: β -PbO₂(Ti)/Na₂SO₄ (0.2 M), O₂-saturated solution, 40° C (this work). 4: β -PbO₂(Ti)/Na₂SO₄ (0.2 M), H₂-saturated solution, 40° C (this work). 5: O₂/H₂O half-cell reaction, 25° C (theory). 6: H⁺/H₂ half-cell reaction, 25° C (theory).

5.6.1. Open-circuit potential versus pH. The dependence of the steady-state value of the rest potential (open-circuit potential) of porous and compact β -PbO₂(Ti) electrodes on the pH of the Na₂SO₄ solution (0.2 M) is shown in curves 3 and 4 of Fig. 7. It follows from Fig. 7 that the open-circuit potential of the β -PbO₂(Ti)/Na₂SO₄ interface is a mixed potential governed by the kinetics of the Equations 1 and 2:



with Equation 2 being apparently more important (faster) as a potential-determining process than Equation 1.

5.6.2. Galvanostatic anodic charging curves. The galvanostatic anodic charging curves in Na₂SO₄ solution for porous and compact β -PbO₂(Ti) electrodes are shown in Figs 8–11. For comparison, similar charging curves for a smooth,

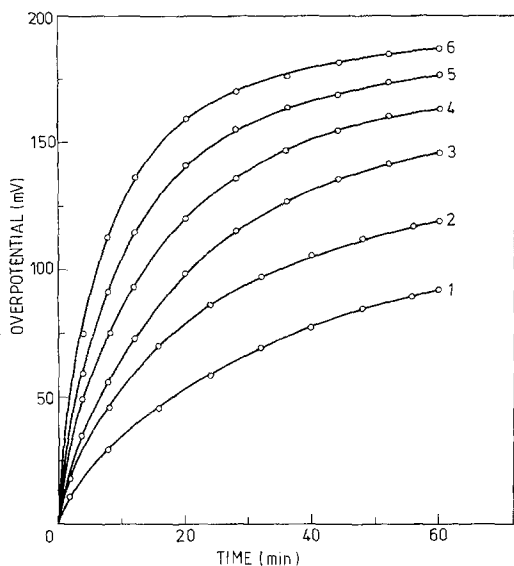


Fig. 8. Galvanostatic anodic charging curves for porous β - $\text{PbO}_2(\text{Ti})$ electrode with PbO_2 coating, 0.5 mm thick, and apparent area 7.8 cm^2 , in contact with Na_2SO_4 (0.2M) solution at 40°C . Charging currents (μA): 1, 40; 2, 60; 3, 80; 4, 100; 5, 140; 6, 180. Overpotential is defined as $E - E_{i=0}$ where E is the electrode potential for a given current, i , at the instant considered, and $E_{i=0}$ is the steady-state open-circuit potential of the electrode in the same solution.

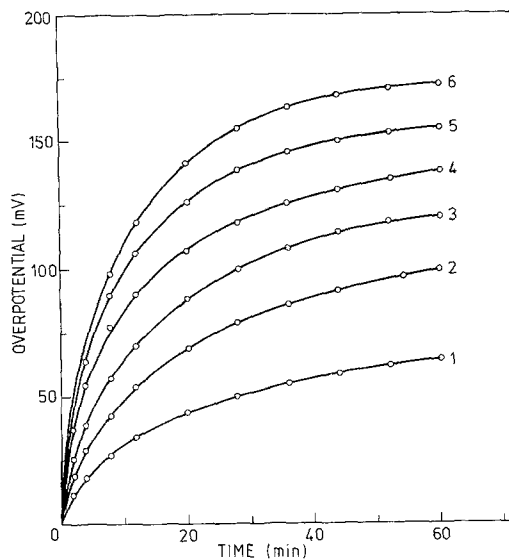


Fig. 10. Galvanostatic anodic charging curves for porous β - $\text{PbO}_2(\text{Ti})$ electrode with PbO_2 coating, 1.0 mm thick, and apparent area 8.0 cm^2 , in contact with Na_2SO_4 (0.2M) solution at 40°C . Charging currents (μA): 1, 100; 2, 140; 3, 180; 4, 220; 5, 260; 6, 300. Overpotential is defined as in Fig. 8.

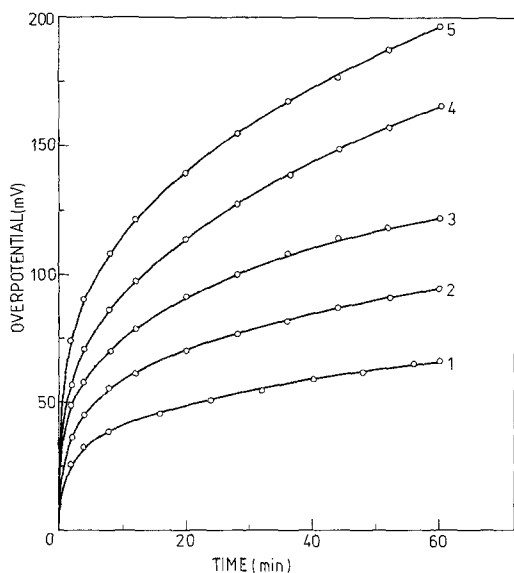


Fig. 9. Galvanostatic anodic charging curves for compact β - $\text{PbO}_2(\text{Ti})$ electrode with PbO_2 coating, 0.5 mm thick, and apparent area 7.6 cm^2 , in contact with Na_2SO_4 (0.2M) solution at 40°C . Charging currents (μA): 1, 15; 2, 20; 3, 25; 4, 30; 5, 40. Overpotential is defined as in Fig. 8.

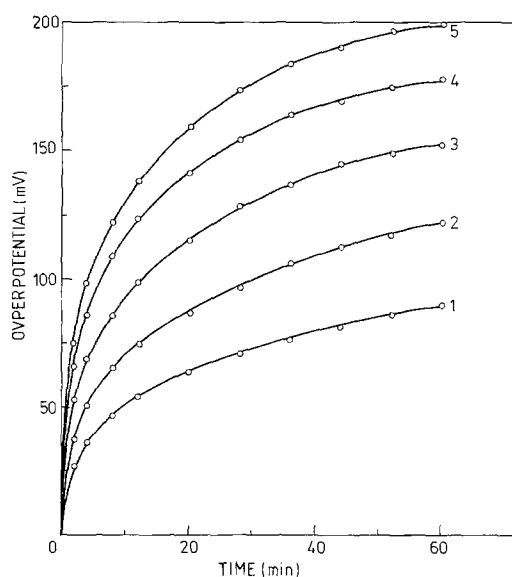


Fig. 11. Galvanostatic anodic charging curves for compact β - $\text{PbO}_2(\text{Ti})$ electrode with PbO_2 coating, 1.0 mm thick, and apparent area 8.0 cm^2 , in contact with Na_2SO_4 (0.2M) solution at 40°C . Charging currents (μA): 1, 20; 2, 30; 3, 40; 4, 50; 5, 60. Overpotential is defined as in Fig. 8.

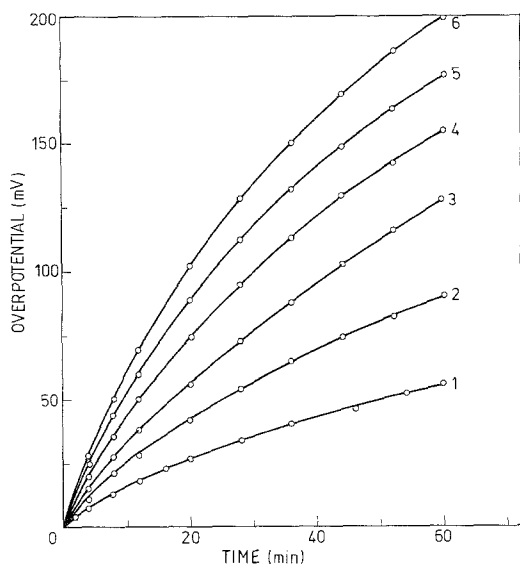


Fig. 12. Galvanostatic anodic charging curves for platinized titanium electrode (area = 6.5 cm²) in contact with Na₂SO₄ (0.2M) solution at 40° C. Charging currents (μA): 1, 1.0; 2, 1.5; 3, 2.0; 4, 2.5; 5, 3.0; 6, 3.5. Overpotential is defined as in Fig. 8.

platinized titanium electrode obtained under otherwise identical conditions are presented in Fig. 12.

The primary objective of the analysis was to obtain the values of the double-layer capacitance at the test electrode as a function of the electrode potential. Since the charging curves are generally distorted due to the occurrence of faradaic reactions, such as that of anodic oxygen evolution, a correction for the faradaic currents is required to obtain reliable results. This may be carried out as follows.

In general, the current density, i , at an electrode is given by

$$i = i_{\text{ch}} + i_{\text{far}} \quad (3)$$

where i_{ch} is the current density for charging the double layer (non-faradaic current density) and i_{far} is the current density corresponding to any charge transfer reaction at the interface.

With due regard to signs[†],

$$i = -C_d \frac{dE}{dt} + i_{\text{far}} \quad (4)$$

[†] Cathodic currents are positive. Electrode potentials are according to the International Convention.

where C_d is the differential capacitance of the electrical double layer at the electrode potential, E .

Allowing for the possibility that C_d may vary with electrode potential, it may be evaluated from experimental charging curves at different currents and at any chosen value of E^* from Equation 4 as follows:

$$C_{d,E^*} = \frac{i_2 - i_1}{\left(\frac{dE}{dt}\right)_{1,E^*} - \left(\frac{dE}{dt}\right)_{2,E^*}} \quad (5)$$

where $(dE/dt)_{1,E^*}$ and $(dE/dt)_{2,E^*}$ are the derivatives of the galvanostatic charging curves at current densities i_1 and i_2 , respectively, each being obtained at E^* (Fig. 13).

Such a procedure has several advantages: it eliminates uncertainties caused by the usually-adopted measurement at $t \rightarrow 0$; it permits a multi-point analysis; it provides information on the dependence of double-layer capacity on potential, and allows a proper correction to be made for faradaic currents without any specific model for the same. (A similar procedure has been adopted earlier [21] using galvanostatic charging curves and subsequent open-circuit polarization decay curve.) However, any adsorption pseudocapacity, if present, is included in the value of $C_{d,E}$ obtained as above.

Accordingly, the charging curves in Figs 8–12 were plotted on a large-scale graph, smooth

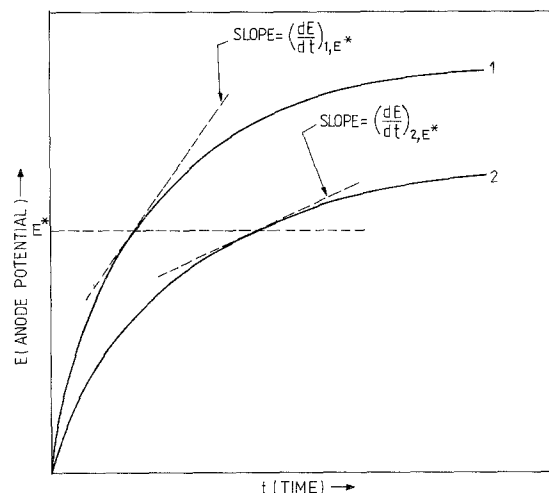


Fig. 13. Schematic diagram of galvanostatic charging curves at two currents (1, 2) and the location of the derivatives at a chosen electrode potential, E^* .

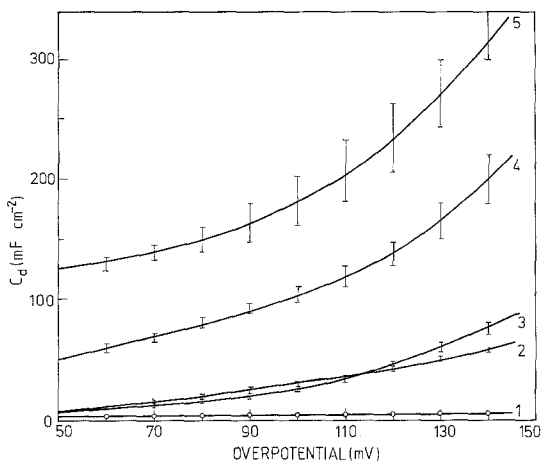


Fig. 14. The dependence of the differential capacitance of the double layer on electrode overpotential in Na_2SO_4 (0.2M) solution of pH 6 at 40°C . 1: Smooth, platinized titanium electrode (no PbO_2 coating). 2: Compact $\beta\text{-PbO}_2(\text{Ti})$ electrode with PbO_2 coating, 0.5mm thick. 3: Compact $\beta\text{-PbO}_2(\text{Ti})$ electrode with PbO_2 coating, 1.0mm thick. 4: Porous $\beta\text{-PbO}_2(\text{Ti})$ electrode with PbO_2 coating, 0.5mm thick. 5: Porous $\beta\text{-PbO}_2(\text{Ti})$ electrode with PbO_2 coating, 1.0mm thick. Overpotential is defined as in Fig. 8. Differential capacitance density is based on apparent area of each electrode.

curves were drawn through the points, and the derivatives required in Equation 5 were obtained by graphical differentiation. The above procedure permitted the determination of C_d at each chosen potential, and then for each of the ten electrode samples studied. The results of such an analysis are summarized and presented in Fig. 14.

Several important conclusions emerge from an inspection of Fig. 14. It follows from curve 1 of Fig. 14 that the double-layer capacitance of a platinized titanium electrode increases only marginally with an increase in potential in the anodic direction. The capacitance value of about 4 mF cm^{-2} near the open-circuit potential increases to about 8 mF cm^{-2} at 120 mV anodic to the open-circuit potential. These values are far higher than the normal double-layer capacitance values in the range of tens of microfarad per cm^2 . Since the area of the smooth, platinized titanium electrode may be assumed to be equal to its geometric area as a good approximation, and contributions from faradaic pseudocapacitance have been eliminated in the above analysis, it follows that the large double-layer capacitance arises due to a strong adsorption of sulphate ions on the Pt(Ti) surface.

Considering now the curves 2 to 5 of Fig. 14, the enhanced capacities of $\beta\text{-PbO}_2(\text{Ti})$ electrodes in comparison with Pt(Ti) electrodes may be attributed to a proportionate increase in the effective area of the electrodes, since a strong adsorption of sulphate ions is known to be present in all the above cases.

The area-enhancement factor, as calculated from the capacitance data near the open-circuit potentials (due to the relative constancy of capacitance with potential in this region), is about 40 for a porous $\beta\text{-PbO}_2(\text{Ti})$ electrode with a 1 mm coating, about 15 for a porous $\beta\text{-PbO}_2(\text{Ti})$ electrode with a 0.5 mm coating and only about 2 for a compact $\beta\text{-PbO}_2(\text{Ti})$ electrode with a 1 mm or 0.5 mm coating, assuming that the capacitance value of 4 mF cm^{-2} for the smooth platinized titanium electrode corresponds to a surface of zero roughness. In other words, when compared with compact $\beta\text{-PbO}_2(\text{Ti})$ electrodes with coatings 1 mm or 0.5 mm thick, the area-enhancement factor is about 20 for a porous $\beta\text{-PbO}_2(\text{Ti})$ electrode with a 1 mm coating and about 7 for a porous $\beta\text{-PbO}_2(\text{Ti})$ electrode with a 0.5 mm coating.

These data indicate that the electrochemically active area of a porous $\beta\text{-PbO}_2(\text{Ti})$ electrode is much larger than that of a compact $\beta\text{-PbO}_2(\text{Ti})$ electrode, and that the effective area increases with thickness in the case of porous $\beta\text{-PbO}_2(\text{Ti})$ electrodes but is nearly independent of thickness in the case of compact $\beta\text{-PbO}_2(\text{Ti})$ electrodes.

5.6.3. Tafel plots for anodic oxygen evolution. A comparison of the porous $\beta\text{-PbO}_2(\text{Ti})$ and the compact $\beta\text{-PbO}_2(\text{Ti})$ electrodes has been made under anodic polarization in Na_2SO_4 solution in the Tafel region. Under these conditions the only possible anodic reaction is that of oxygen evolution reaction.

The steady-state Tafel plots for oxygen evolution reaction obtained point-by-point under galvanostatic polarization for the two types of electrodes are shown in Fig. 15. It may be seen that good Tafel plots of slope about 150 mV and extending over two decades of current (0.05 mA cm^{-2} to 5.0 mA cm^{-2}) are obtained in all the four cases.

The exchange current density for the oxygen evolution reaction is readily obtained by extrapolating the well-defined Tafel lines in the low

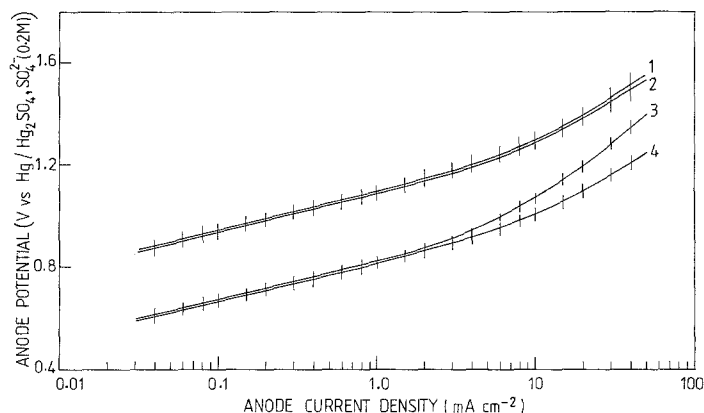


Fig. 15. Steady-state Tafel plots for oxygen evolution reaction on: (1) compact $\beta\text{-PbO}_2(\text{Ti})$ electrode with a 0.5 mm coating; (2) compact $\beta\text{-PbO}_2(\text{Ti})$ electrode with a 1.0 mm coating; (3) porous $\beta\text{-PbO}_2(\text{Ti})$ electrode with a 0.5 mm coating; and (4) porous $\beta\text{-PbO}_2(\text{Ti})$ electrode with a 1.0 mm coating in contact with Na_2SO_4 (0.2 M) solution at 40°C . Each curve is obtained with four electrodes, the range of data being shown by the vertical lines. Current density is based on the apparent area of each electrode.

current density region (below 1.0 mA cm^{-2}) to the reversible potential, namely 0.178 V versus $\text{Hg}/\text{Hg}_2\text{SO}_4$, $0.2\text{ M Na}_2\text{SO}_4$. The values of the exchange current density thus derived from Fig. 15 are about $0.03\text{ }\mu\text{A cm}^{-2}$ for the porous $\beta\text{-PbO}_2(\text{Ti})$ electrode (0.5 mm or 1 mm thick), and about $0.002\text{ }\mu\text{A cm}^{-2}$ for the compact $\beta\text{-PbO}_2(\text{Ti})$ electrode (0.5 mm or 1 mm thick). In other words, the porous $\beta\text{-PbO}_2(\text{Ti})$ electrode is about 15 times more active electrocatalytically than the compact $\beta\text{-PbO}_2(\text{Ti})$ electrode for oxygen evolution reaction under the same conditions.

Though there is some deviation from the Tafel line at higher current densities, which is probably caused by the shielding of gas bubbles (since there is no mass transfer control in this region as was established by an additional stirring of the electrolyte), the electrocatalytic effect of the porous $\beta\text{-PbO}_2(\text{Ti})$ electrodes (0.5 mm and 1.0 mm thick) is clearly seen under practical conditions of higher current densities. Thus, at 1.2 V (versus $\text{Hg}/\text{Hg}_2\text{SO}_4$, $0.2\text{ M Na}_2\text{SO}_4$), the anodic current for a porous $\beta\text{-PbO}_2(\text{Ti})$ electrode with a 0.5 mm coating (curve 3 of Fig. 15) is five times that for a compact $\beta\text{-PbO}_2(\text{Ti})$ electrode with a 0.5 mm coating (curve 1 of Fig. 15). Similarly, the anodic current for a porous $\beta\text{-PbO}_2(\text{Ti})$ electrode with a 1.0 mm coating (curve 4 of Fig. 15) is eight times that for a compact $\beta\text{-PbO}_2(\text{Ti})$ electrode with a 1.0 mm coating (curve 2 of Fig. 15). Although this enhancement in electrocatalytic activity is not in direct proportion to the area enhancement factors deduced above from capacitance data, the improvement is significant.

Considering that the area ratio of the two electrodes as deduced from the double-layer capacitance data is of the same order of magnitude as the ratio of exchange current densities on these electrodes, the enhanced electrocatalytic activity of porous $\beta\text{-PbO}_2(\text{Ti})$ anodes may be expected to prevail also for other reactions of electrosynthesis. Moreover, it is likely that the advantage is realized without any loss of durability of the anode, since the substrate-side of the porous $\beta\text{-PbO}_2(\text{Ti})$ electrodes could be obtained practically non-porous while the other side exposed to solution remains porous.

6. Conclusions

It is possible to deposit adherent coatings of lead dioxide with controlled porosity on a titanium substrate covered by a conducting interphase, such that the porosity in the lead dioxide coating is manifest mainly on the side of the solution. An important consequence is that there is a substantial enhancement of the effective area of the anode without loss of mechanical strength. The low effective current density on such anodes leads to a substantial decrease of the anode overpotential and therefore of cell voltage. The exterior porosity of the anodes may be expected to relieve any internal stress and thereby increase their durability in electrosynthetic applications.

Acknowledgement

Financial support by ISRO through a RESPOND

project to a part of this work is gratefully acknowledged.

References

- [1] J. P. Carr and N. A. Hampson, *Chem. Rev.* **72** (1972) 679.
- [2] H. Bode, 'Lead-Acid Batteries' (translated by R. J. Brodd and K. V. Kordesch), John Wiley & Sons, New York (1977).
- [3] M. A. Dasoyan and I. A. Aguf, 'Current Theory of Lead Acid Batteries', Technicopy Ltd, Gloucester (1979).
- [4] K. V. Kordesch, 'Batteries, Vol. 2: Lead-Acid Batteries and Electric Vehicles', Marcel Dekker, Inc. New York (1977).
- [5] G. H. Kelsall, Electricity Council Research Centre Report, N1060, June (1977).
- [6] G. H. Kelsall and R. Stevens, Electricity Council Research Centre Report, M1266, July (1979).
- [7] A. T. Kuhn and P. M. Wright, in 'Industrial Electrochemical Processes' (edited by A. T. Kuhn), Elsevier (1971) chap. 14.
- [8] D. Gilroy and R. Stevens, *J. Appl. Electrochem.* **10** (1980) 511.
- [9] J. C. Grigger, H. C. Miller and F. D. Loomis, *J. Electrochem. Soc.* **105** (1958) 100.
- [10] R. Stevens and D. Gilroy, *J. Microscopy* **124** (1981) 265.
- [11] Ch. Comninellis and E. Plattner, *J. Appl. Electrochem.* **12** (1982) 399.
- [12] D. Gilroy, *ibid.* **12** (1982) 171.
- [13] F. Hine, M. Yasuda, T. Iida, Y. Ogata and K. Hara, *Electrochim. Acta* **29** (1984) 1447.
- [14] A. T. Kuhn, 'The Electrochemistry of Lead', Academic Press, London (1979).
- [15] F. Hine, M. Yasuda, T. Iida, Y. Ogata and K. Hara, *Electrochim. Acta* **29** (1984) 1447.
- [16] W. Mindt, *J. Electrochem. Soc.* **116** (1969) 1076.
- [17] B. N. Kabanov, E. S. Weisberg, I. L. Romanova and E. V. Krivolapova, *Electrochim. Acta.* **9** (1964) 1197.
- [18] P. C. Foller and C. W. Tobias, *J. Electrochem. Soc.* **129** (1982) 567.
- [19] F. Hine, M. Yasuda, T. Noda, T. Yoshida and J. Okuda, *J. Electrochem. Soc.* **126** (1979) 1439.
- [20] M. A. Dasoyan and I. A. Aguf, 'Current Theory of Lead-Acid Batteries', Technicopy Ltd, Gloucester (1979) p. 39.
- [21] R. Ramesham, PhD dissertation, Indian Institute of Science, Bangalore (1983).